Selection and Characterization of River Fugitive Dust Episodes over Zhuoshui River in Taiwan

I-Cheng Chang[1], Yu-Chun Chiang[2],Tai-Yi Yu[3*]

[1]Department of Environmental Engineering, National Ilan University, 1 Sec. 1, Shennong Rd., Yilan City, Yilan County 260, Taiwan

[2]Department of Mechanical Engineering, Yuan Ze University, 135 Yuan-Tung Road, Chung-Li, Taiwan 320, Taiwan

*[*3]Department of Risk Management and Insurance, Ming Chuan University, 250 Zhong Shan N. Rd., Sec. 5, Taipei 111, Taiwan*

Abstract

This study employs principal component analysis to cite river fugitive dust episodes over Zhuoshui River in Taiwan. The component scores of the first principal component were applied as the indicators to screen the river fugitive dust episodes. As for the daily PM_{10} concentrations at monitoring stations in Zhuoshui River, the first principal component explains 65% of total variance of concentrations. As for the principal components behind the first principal component, since the contributions of PM_{10} concentrations was lower than 13%, they were not suitable indicators for selecting air pollution episodes. The numbers of days exceeding national ambient air quality standard (NAAQS) for PM_{10} was used to evaluate effectiveness for the component scores of the first principle component. In selecting river fugitive dust episodes, the polluted episodes resulted from dust storms and transboundary pollution cannot be sieved as target episodes. The features of meteorological parameters, synoptic weather, PM_{10} concentrations and principal components of

principal components for river fugitive dust episodes over Zhuoshui River were also analyzed as useful references to forecast river fugitive dust episodes and implement related air quality management issues.

Keywords: principal component analysis, synoptic weather, river fugitive dust

1. Introduction

In Taiwan, the base flow of certain rivers has dropped sharply because of topographic characteristics of drainage basins, climate change, water resource allocation, watershed management, and riverbank reclamation and development. After the 1999 Jiji earthquake, riverbeds were raised and exposure of downstream riverbeds increased. Furthermore, after typhoons, a large amount of debris is flushed down rivers from upstream; this occurs during the northeast monsoon season, resulting insubstantially elevated levels of dust emissions. According to air quality monitoring conducted by the Taiwan Environmental Protection Administration (TEPA), dust episodes primarily occur from October to April of the following year. In addition to reducing the quality of life of and causing inconvenience for residents of downwind areas, dust episodes may affect residents' physical and mental health. As well as long-term changes in the natural environment, possible causes of river dust include part of the riverbed gravel being exposed when a dry spell occurs during a strong northeast monsoon in winter; moreover, when farmers do not suppress dust carefully, river dust may be generated when the farmers use riverbanks during periods of fallowing, planting, and turning. Recently, numerous river dust-related grievances have been filed with the Taiwanese government in the surrounding basins of the Zhuoshui, Beinan, Daan, and Dajia Rivers, indicating that river dust emissions are a

serious problem. Take Syuguang station as an example, a river dust monitoring station along the Zhuoshui River; the maximum daily average concentration of PM_{10} (particulate matter of 10μm in diameter) appeared on October 22, 2013 (417 μg m^{-3}), during which the maximum 1-hour concentration was 1102 μg m^{-3}.

Screening for episodes of air pollution is essential preparation work for formulating regulations on air pollution, air quality simulation, and air quality management. In particular, simulating secondary air pollutants and related topics require great resources to process the complex physical and chemical reactions involved. Simulation calculations can be simplified and time saved by using representative air pollution episodes. Additionally, verifying the simulation results of air quality models through air quality monitoring data can facilitate analysis and understanding of the causality between numerous factors such as air quality, weather, pollution sources, and topography. Conventional screening of air pollution scenarios begins with classifying meteorological patterns and preparing relevant statistics. The classification of meteorological patterns must rely on meteorological data and the professional capability of meteorological experts. However, because the determination of classification methods and methods of expert assessment are not unified, the classification of meteorological patterns cannot demonstrate the statistically extreme concentration of pollutants. The statistical methods used for meteorological patterns often adopt extreme values and the exceedances of ambient air quality as screening standards. When using extreme values, the statistical methods often cannot derive consistent results for numerous monitoring stations due to their differing characteristics.

Regarding the classification of meteorological patterns, the United States Environmental Protection Agency (U.S.EPA, 1991) selected meteorological conditions that were prone to high ozone and then selected the 3 days with the most severe ozone pollution levels in each meteorological pattern to define an ozone episode. Cassmassi (1999) used synoptic weather

patterns and atmospheric stability to establish the Meteorological Potential of Atmospheric Pollution (PMCA) index, and adopted multivariate regression tools to predict PM_{10} episodes. Perez and Reyes (2002) used a neural network to predict PM_{10} episodes and found that temperature difference between day and night was a crucial factor in specific meteorological patterns. Regarding statistical research on monitoring values, Ames *et al.* (1985) selected episodes based on a frequency of not more than 10 times in 3 years (3 times a year); permissible concentration was also used to determine an episode. Meyer *et al.* (1997) attempted to simulate the maximum 8-hour ozone values from June 1 to August 31, 1987 using the Regional Oxidant Model, and selected meteorological conditions with high concentrations of pollutants, identifying these as ozone episodes. However, the three-dimensional grid air quality model entails high resource costs, which is unsuitable as a tool for determining an immediate pollution episode. Using the aforementioned meteorological classifications, extreme values statistical methods, and air quality models is not feasible for instantly selecting appropriate and statistically representative pollution scenarios. In terms of using statistical methods to screen pollution episodes, Yu and Chang (2000) and Yu (2013) adopted principal component analysis (PCA) to screen ozone pollution and PM_{10} episodes, respectively. Kuebler *et al.* (2002) used classification and regression tree analysis to screen ozone episodes on the Swiss Plateau. Beaver and Palazoğlu (2006) adopted K-mean cluster analysis to screen ozone episodes in California. Zhang *et al.* (2014) used PCA and a nonparametric T^2 control chart to predict episodes of over-standard ozone concentrations. Sun *et al.* (2015) predicted over-standard ozone episodes by adopting generalized linear mixed effects models (GLMMs). In the same study, the researchers compared the difference between linear regression models, generalized linear models, multilayer perceptron, and support vector machines, and found that GLMMs provided predictions with lower prediction errors and more correct over-standard ozone episodes for various weather patterns.

In the field of air pollution research, PCA is an effective and objective data analysis tool that is often used to simplify variables(Yu and Chang, 2006; Dai *et al.*, 2015; Iodice *et al.,* 2016; Yao *et al.*, 2016; Chen *et al.*, 2017), identify sources of pollution (Viana *et al.*, 2006; Shi *et al.*, 2009; Deka *et al.*, 2014; Huang *et al.*, 2015; Luo *et al.*, 2015; Mari *et al.*, 2016; Arhami *et al.*, 2017), classify meteorological patterns (Maheras P., 1984; Maryon and Storey, 1985; Eder *et al.*, 1994; Cheng and Lam, 2000), and evaluate model diagnostics (Eder *et al.*, 2014; Li and Wen., 2014). Researchers can use large amounts of existing monitoring data to instantly select statistically representative air pollution scenarios and, in particular, provide consistent high concentrations of air pollutants at most stations. These data can serve as a decision-making reference for formulating future strategies on air quality management to screen for air pollution episodes. The PCA has two advantages; first, it simplifies the relevant variables of air pollution to achieve economic effectiveness; and second, for screening pollution episodes, it exhibits more objective statistical representativeness than the meteorological classification. For screening river dust episodes, this study adopted the research method of Yu and Chang (2000) and Yu (2013). Based on air quality monitoring data, this study adopted PCA to screen pollution episodes, and then analyzed the air quality and meteorological characteristics of dust episodes. Finally, the appropriateness of the screening process was evaluated.

2. Research Methods

2.1 Air quality data

The Taiwan Air Quality Monitoring Network was officially launched by the TEPA in September 1993. To date, 76 general stations, 63 regular stations, 4 industrial stations, 2 national park stations, 4 background stations, and 6 traffic stations have been installed. The following five

stations are located along the Zhuoshui River basin: Jushan, Douliou, Lunbei, Mailiau, and Taishi. The monitoring parameters are SO_2, CO, O_3, PM_{10}, NO, NO_2, NMHC, THC, $PM_{2.5}$, wind speed, wind direction, temperature, and relative humidity. The Zhuoshui River is the longest river in Taiwan with the largest amount of sediment, and its upstream tributaries carry a large amount of sediment from the mountains, depositing into the estuary (Dadson *et al.*, 2003). Its estuary is a wide and braided channel with numerous exposed sandbars. During the winter dry spell, these sandbars easily form a large bare area. Coupled with the prevalence of the northeast monsoon, PM_{10} levels are elevated by wind, leading to serious river dust disasters in the downwind areas of the south bank of the Zhuoshui River. In Taiwan, river dust episodes usually occur during the dry spell of the northeast monsoon season (from October to April of the following year). In addition to general air quality stations, the TEPA has established automatic PM_{10} monitoring equipment near rivers that commonly have river fugitive dust, to understand river dust conditions and forecast air quality. High PM_{10} concentrations are likely to be detected by the monitoring stations near riverbeds because dust accumulated on the riverbed generates dust emissions when blown by strong wind. River dust data measured by a monitoring station can only represent the influence of dust in the local area and cannot represent regional air quality. The TEPA established two stations at Yisian and Syuguang Elementary Schools. Along the Zhuoshui River basin, five parameters are monitored: PM_{10}, wind speed, wind direction, temperature, and relative humidity. To simultaneously evaluate the effect of river dust on air quality, the air quality monitoring data of this study were taken from the EPA's general and river dust stations from 2011 to 2017. The target area was the Zhuoshui River basin, and the following seven stations were included: Jushan, Douliou, Yisian, Syuguang, Lunbei, Mailiau, and Taishi (Fig. 1).

Please insert figure 1 here

This study's primary tasks were as follows:

1. To screen river dust episodes of the Zhuoshui River: This study employed PCA of multivariate statistics to analyze data from the TEPA's air quality and river dust monitoring stations for the Zhuoshui River basin from 2011 to 2017 (data from the river dust monitoring stations began from 2011). The river dust monitoring stations only recorded PM_{10} data; therefore, PM_{10} was the research target and $PM_{2.5}$ was excluded.
2. To mitigate the effects of dust storms and foreign pollution episodes from the screened river dust episodes: Affected by dust storms in Mongolia and foreign air pollutions, the PM_{10} concentration can increase sharply in a short period. Therefore, this study compared dates when dust storms and foreign pollution affected Taiwan and removed PM episodes that may have been caused by dust storms and foreign pollution.
3. To evaluate the appropriateness of episodes for statistical representativeness. Existing data of synoptic weather patterns, meteorology, and PM_{10} concentrations were used to evaluate the appropriateness of pollution episodes.

2.2 Principal component analysis

Monitoring data from air quality stations were analyzed from the EPA's air quality stations. The data period was from 2011 to 2017, and the daily average PM_{10} value was taken as the sample value. The data dimension of PM_{10} could be treated as a collection of time series of 7 vectors (7 stations × 2557 days). Subsequently, the monitoring data were normalized using the following equation:

$$Z_{ik} = \frac{C_{ik} - \mu_i}{S_i}$$

Where Z_{ik} is the score of the *Kth* Z of station I; C_{ik} is the *Kth* pollutant value of station I; μ_i is the average value of station I; and S_i is the standard deviation of station I. The relationship between the standardized Z-score and the nonrotating principal component value is as follows:

$$Z_{ik} = \sum_{j=1}^{n} L_{ij} P_{jk}$$

Where L_{ij} is the factor loading of the *Jth* principal component of station I; and P_{jk} is the component score of the *Kth* variable in the *Jth* principal component. The score of the principal component can be derived using the inverse matrix of the aforementioned formula.

$$P_{jk} = \sum_{i=1}^{n} (L_{ij} / \lambda_j) Z_{ik}$$

Where λ_j is the eigenvalue of the *Jth* principal component and also represents the variance of the *Jth* principal component. All of the principal components are arranged based on the order of their explained variance from greatest to least; therefore, using the first few principal components enables the grasping of most of the variance in the entire sample space and achieves the simplification of variables. The principal components of these linear combinations exhibit not only the smallest variance in their components, but also the maximum individual differences of the individual components. Therefore, the first principal component can explain the maximum variation in the concentration field. This study screened appropriate river dust episodes using the characteristics of the first principal component.

3. Results and Discussions

3.1 Geographical distribution of PM_{10} concentrations during dry season

The highest monthly average of PM_{10} daily average values (Figure 2) from the monitoring

184 stations in the Zhuoshui River basin occurred in November, followed by December and March.
185 The monthly mean PM_{10} during the dry season at all monitoring stations was substantially higher
186 than that during the wet season. The difference in the monthly average concentrations during the
187 wet and dry seasons was approximately 30–45μg m^{-3}. The monitoring results from the river dust
188 monitoring stations at Yisian and Syuguang Elementary Schools were compared, as shown in
189 Figure 3a. At Syuguang, the cumulative probability density distribution indicated that differences
190 in PM_{10} concentration during wet and dry seasons at 25%, 50%, and 75% cumulative probability
191 were 21, 30, and 40μg m^{-3}, respectively; at Yisian, they were 21, 31, and 40μg m^{-3}, respectively.
192 otably, the difference in extremely high PM_{10} concentrationsat Syuguang was much higher than
193 those at Yisian. According to the locations of the stations and the Zhuoshui River, both stations
194 were located on the south bank of the river. From the difference in PM_{10} concentrations between
195 wet and dry seasons, the difference was consistent at less than 90% cumulative probability;
196 however, for extremely high PM_{10} concentrations, the river dust exhibited greater influence at
197 Syuguang than at Yisian. For the differences in PM_{10} concentrations betweenwet and dry seasons
198 at the TEPA's general stations, the two sites exhibiting the largest difference—Taishi and
199 Mailiau—were selected for comparison (Figure 3b). The cumulative probability density of
200 difference in PM_{10} concentration during the wet and dry seasons at Taishi were 19, 26, and 30 μg
201 m^{-3} at the cumulative probabilities of 25%, 50%, and 75%, respectively; those at Mailiau were 25,
202 33, and 37μg m^{-3}, respectively. However, the cumulative probability density of 90% and 95% for
203 PM_{10} difference (the difference in PM_{10} concentrations for wet and dry seasons) were 37 and 56
204 μg m^{-3} in Taishi; and 42 and 80 μgm^{-3} in Mailiau. Compared with the aforementioned seven
205 stations, river dust was found to exhibit the greatest influence on the closest stations at Syuguang
206 and Yisian on the south bank of the Zhuoshui Riverbed, followed by the Mailiau and Taishi
207 Stations.

Please insert Figure 2 here

Please insert Figure 3 here

3.2 PCA

PCA was performed based on the daily average PM_{10} concentration from the seven stations. The results (Table 1) showed that the eigenvalues of the first three principal components were 4.57, 0.89, and 0.55, respectively, and the explanation for the concentration variance was 65.3%, 12.7%, and 7.9%, respectively. Therefore, the first unrotated principal component accounted for 65.3% of the variance in PM_{10} concentration. The factor loading value represented the correlation between the principal component and each station. From the factor loading of each station and the first principal component (Table 2), the top three stations exhibiting the highest factor loadings of the first principal component were Douliou (0.888), Lunbei (0.848), and Taishi (0.834). The factor loading of each station and the first principal component was higher than 0.72. For the absolute value of the factor loading of the second principal component, only Jushan exhibited a value higher than 0.5.

Please inert Table 1 here

Please inert Table 2 here

If the first unrotated principal component exhibited a high value, the concentration of all stations would collectively increase. Therefore, to understand harmful river dust episodes, the numbers of exceedance (in 1 day, if one station detected a PM_{10} concentration higher than daily mean PM_{10} standard, the number of exceedance was 1; if it was two stations, the number was 2) for PM_{10} was

selected and the component scores of the first principal component were compared. As for the standard, this study selected two criteria: 150 and 125μg m^{-3} (150 was STN1 and 125 was STN2). According to the results in Figure 4, the higher the component score of the first principal component, the higher the numbers of exceedance there were. The results of the analysis were as follows:

1. The component score of the first principal component that was higher than 1 accounted for 13.5%, and could screen for 78.9% of exceedance with PM_{10} concentrations exceeding 125μg m^{-3}. The average number of exceedance was 1.89. The component score could screen for 85.0% of exceedance with PM_{10} concentrations exceeding 150μg m^{-3}, and the average number of exceedance was 0.88.
2. The component score of the first principal component that was higher than 2 accounted for 3.30% and could screen for 42.3% of exceedance with PM_{10} concentrations exceeding 125μg m^{-3}. The average number of exceedance was 4.14. The component score could screen for 60.4% of exceedance with PM_{10} concentrations exceeding 150μg m^{-3}, and the average number of exceedance was 2.55.

Please inert Figure 4 here

In addition to assess the relationships between component scores of the first principal component and numbers of PM_{10} episodes detected by monitoring stations, this study evaluated synoptic weather patterns (Soong *et al.*, 2005), wind speed, wind direction, height of mixing layer (Air Quality Modeling Center, TEPA, 2018), and ventilation index (wind speed recorded in Wuqi Weather Station, CWB× height of mixing layer; Air Quality Modeling Center, TEPA, 2018).

253 Therefore, according to existing monitoring data, parameters such as the PM_{10} concentration,
254 ventilation index, and height of mixing layer exhibited low degrees of correlation. No moderate
255 positive correlation (0.4–0.7) was found amongthese parameters. The correlation between wind
256 speed, wind direction, and PM_{10} concentration was investigated. The number of exceedance for
257 PM_{10} standard in each year was compared, and the highest number of exceedance occurred in
258 2013 (100 times) and 2014 (121 times). The station with the most severe PM_{10} concentration in
259 2013 was Syuguang (23 times). The highest PM_{10} concentration recorded by Syuguang was in
260 October. Therefore, the hourly concentration, wind speed, and wind direction in October 2013
261 were analyzed to realize correlationships between these parameters. The most severe PM_{10}
262 episode detected by Syuguang in October 2013 was October 21-27. During this period, the air
263 quality was also affected by Typhoon Francisco and Typhoon Lekima. The relationship between
264 the hourly PM_{10} concentration and wind speed at Syuguang was analyzed during these two
265 selected periods. The relationship between hourly PM_{10} concentration and wind speed at
266 Syuguang in October 2013 (Figure 5a) and October 21–27, 2013 (Figure 5b) demonstrated that
267 the hourly PM_{10} concentration and wind speed did not exhibit favorable linear or quadratic
268 correlations. The relationship between hourly wind direction and hourly PM_{10} concentration at
269 Syuguang in October 2013 and the average PM_{10} concentration at every time period are shown in
270 Figures 5c and 5d. The hourly wind direction in Figure 5c shows that in October 2013, wind
271 directions with PM_{10} concentrations higher than 200 $\mu g\ m^{-3}$ were from the north, northeast, and
272 northwest, whereas PM_{10} concentrations higher than 400 $\mu g\ m^{-3}$ were only from the north and
273 northwest. Syuguang is located on the south bank of the Zhuoshui River; thus, the air quality at
274 Syuguang was obviously affected by river fugutive dust. As for the periods of high PM
275 concentration and high wind speed (Figure 5d), they all occurred at approximately 15:00 and
276 16:00. Therefore, high wind speeds resulted in high PM_{10} concentrations during river dust

episodes.

Please inert Figure 5 here

To evaluate the effectiveness of screening river dust episodes, daily mean PM_{10} values exceeding 125 and 150 μg m^{-3} were compared. The numbers of exceedance for PM_{10} standard (over 125 μg m^{-3}), which was more statistically representative (the number of exceedance was 497 in 2011–2017). The primary stages of principles for screening river dust episodes are as follows: (1)During the monitoring period, 1 day occurs where the component score of the first principal component is higher than 3; (2)Dust storms and transboundary pollution are eliminated；(3)The component score of the first principal component is higher than 1 for five 5 consecutive days.

According to the first stage, the total number of days that the score of the first principal component was higher than 3 was 18 days. The results of screened PM_{10} concentrations at stations are shown in Table 3. The highest score of the first principal component was found on January 21, 2014 and the component score of the first principal component was 6.05. The daily average PM_{10} concentration value was 345 μg m^{-3}at Syuguang and 368 μg m^{-3} at Taishi. For the second stage, the dates of dust storms and transboundary pollution were compared. During the 18 days, except for October 22, October 25, and October 13, 2017, which were affected by the three typhoons Francisco, Lekima, and Khanun, respectively, the high PM_{10} concentrations on the remaining dates were caused by transboundary pollution. According to the third stage, river dust episodes that exhibited a component score of the first principal component higher than 1 for 5 consecutive days were selected. Therefore, only the dust episodes during October 22–26, 2013 could be selected. To provide multiple choices, the score of the first principle component was

modified to be higher than 2, enabling three alternative episodes to be selected (Table 4). Synoptic weather patterns were an essential factor that affected air quality; the cross-correlation among PM_{10} concentrations, principal components, and synoptic weather patterns was explored. The monitoring results from Syuguang (Table 5) indicated the following: (1)The first three synoptic weather patterns exhibiting the highest daily PM_{10} concentrations were northeast monsoon and peripheral circulation of the typhoon, peripheral circulation of the typhoon, and high-pressure circulation mixing with a warm sector. The average wind speeds of the three weather patterns recorded at Lunbei were 3.7, 3.0, and 1.9 m/s, respectively. (2)The average wind speed and PM_{10} levels of strong northeast monsoons, standard northeast monsoons, and weak northeast monsoons were compared. The strong northeast monsoon exhibited the highest average wind speed (4.0 m/s) and the highest PM_{10} concentration. The six stations all exhibited these characteristics except for Lunbei. (3)Regarding the weather pattern of the northeast monsoon and peripheral circulation of the typhoon, Syuguang, Mailiau, Taishi, and Douliou Stations exhibited the highest average PM_{10} concentrations. (4)The top three synoptic weather patterns exhibiting the highest component scores of the first principal component were the northeast monsoon and peripheral circulation of the typhoon, high-pressure circulation mixing with a warm sector, and high-pressure recirculation. Whether high-pressure recirculation and wind speed severely influence river fugitive dust will be examined later. (5)For the synoptic weather pattern exhibiting the highest PM_{10} concentration, a strong northeast monsoon was determined to carry the highest PM_{10} concentration at Mailiau, Pacific high pressure stretching westerly at Yisian, and high-pressure recirculation at Lunbei.

Please insert table 3 here

Please insert table 4 here

Please insert table 5 here

In addition to considering synoptic weather patterns, a cross-analysis was conducted to carefully evaluate the correlation between the scores of the first principal component, weather patterns, and wind speeds at Lunbei (wind speed was divided into high and low wind speeds at 3.5m/s) (Table 6). The findings were as follows: (1)High wind speed elevated the componet score of the first principal component of weather patterns including the Northeast monsoon and peripheral circulation of the typhoon, Peripheral circulation of the typhoon, strong northeast monsoon, and the Pacific high pressure. That is, these four synoptic weather patterns increased the PM_{10} concentration at each station under the condition of high wind speed. (2)Comparing a standard northeast monsoon with a weak northeast monsoon, the component score of the first principal component of high wind speed was not necessarily higher than that of low wind speed. (3)In the Zhuoshui River basin, river dust episodes were easily formed in the aforementioned four synoptic weather patterns at high wind speeds. Northeast monsoon and peripheral circulation of the typhoon as well as Peripheral circulation of the typhoon were directly related to typhoons. Based on previous synoptic weather patterns, the Pacific high and Pacific high pressure stretching westerly exhibited higher scores in the first principal component. The Pacific high and Pacific high pressure stretching westerly often occurred at 1 day before or after two weather patterns of Northeast monsoon and peripheral circulation of the typhoon and Peripheral circulation of the typhoon. (4)A typhoon that affected Zhuoshui River areas was usually accompanied by rainfall, and the rainfall reduced the PM concentration.

Relevant studies on river fugitive dust pollution in Taiwan have begun by separating the seasons into wet and dry. However, the present study investigated monitoring data from the Zhuoshui River basin and found that typhoons in July, August, and September still caused local river dust episodes; for example, September 15, 28, and 29, 2012, and October 16–21, 2015. In addition to transboundary pollution (Oh *et al.*, 2015; Lai *et al.*, 2016) and dust storm episodes,

two characteristics—typhoons that did not pass over the land in Taiwan and northeast monsoons during dry season—are also likely to cause river dust episodes in the Zhuoshui River basin. Based on the past experiences, river fugitive dust episodes easily occurred during season at Taiwan, construction period of performing yearly control measures to combat river fugitive dust was then set in September. However, analytical results of this study proposed the typhoon season (often occurred at July-September) (Fang *et al.*, 2009; Cheng and You, 2010) could be another crucial factor to cause river fugitive dust episodes pollution. Therefore, control method and construction period of mitigating river fugitive dust at Taiwan must take into account the typhoon season.

Please insert table 5 here

Conclusion

This study applied unrotated principal component analysis for screening river fugitive dust episodes and analyzed those characteristics of PM_{10} concentrations, synoptic patterns and meteorological parameters in Zhuoshui River, analytic results of river dust episodes could be served as useful references for forecasting air quality. The component score of the first components is an adequate indicator to screen air pollution episodes. The station numbers of exceeding PM_{10} standard increased with the component score of the unrotated first principal component. Beside the PM_{10} episodes resulted from transboundary pollution and dust storm, the dominant three synoptic patterns to cause fugitive river dust episodes in Zhuoshui River are "peripheral circulation of the typhoon" and "northeast monsoon and peripheral circulation of the typhoon" and "strong northeast monsoon". This study identified two conditions to easily cause river fugitive dust episodes; firstly, the typhoon periods that typhoon without landing Taiwan; secondly, "strong northeast monsoon" in the dry season. Except for dry season, analytical results

of multivariate manner demonstrated the typhoon season is the key factor to form river fugitive dust episodes in Taiwan. Consequently, the control method and construction period of mitigating river fugitive dust must take into account the typhoon season.

Acknowledgments

We express our gratitude to the Ministry of Science and Technology of Taiwan (MOST-106-EPA-F-013-001) and Environmental Protection Administration of Taiwan for funding this study.

References

1. Ames, J., Mayers, T.C., Reid, L.E., Whitney, D.C., Goldings, S.H., Hayes, S.R. and Reynolds, S.D. (1985). *Airshed Model Operations Manuals, Vol. I, User's Guide Manual; Vol. II, Systems Manual. EPA-600/8-85/007a, b.* US Environmental Protection Agency, Atmospheric Sciences, Research Laboratory, Research Triangle Park, NC.
2. Arhami, M., Hosseini, V., Shahne, M.Z., Bigdeli, M., Lai, A. and Schauer, J.J. (2017). Seasonal trends, chemical speciation and source apportionment of fine PM in Tehran. *Atmos. Environ.* 153: 70-82.
3. Beaver, S. and Palazoğlu, A. (2006). A cluster aggregation scheme for ozone episode selection in the San Francisco, CA Bay Area. *Atmos. Environ.* 40(4): 713-725.
4. Cassmassi, J. (1999). *Improvement of the forecast of air quality and of the knowledge of the local meteorological conditions in the Metropolitan region*. CONAMA, Santiago, Chile.
5. Chen, Y., Li, X., Zhu, T., Han, Y. and Lv, D. (2017). $PM_{2.5}$-bound PAHs in three indoor and one outdoor air in Beijing: Concentration, source and health risk assessment. *Sci. Total Environ.* 586: 255-264.
6. Cheng, M.C. and You, C.F. (2010). Sources of major ions and heavy metals in rainwater associated with typhoon events in southwestern Taiwan. *J. Geochem. Explor*. 105: 106-116.
7. Cheng, S. and Lam, K.C. (2000). Synoptic typing and its application to the assessment of climatic impact on concentrations of sulfur dioxide and nitrogen oxides in Hong Kong. *Atmos. Environ.* 34(4): 585-594.
8. Dadson, S.J., Hovius, N., Chen, H., Dade, W.B., Hsieh, M.L., Willett, S.D. and Lague, D. (2003). Links between erosion, runoff variability and seismicity in the Taiwan orogen. Nature, 426(6967), 648.

9. Dai, Q.L., Bi, X.H., Wu, J.H., Zhang, Y.F., Wang, J., Xu, H., and Feng, Y.C. (2015). Characterization and source identification of heavy metals in ambient PM_{10} and $PM_{2.5}$ in an integrated iron and steel industry zone compared with a background site. *Aerosol Air Qual. Res*. 15(3): 875-887.

10. Deka, P. and Hoque, R.R. (2014). Diwali fireworks: early signs of impact on PM_{10} properties of rural Brahmaputra valley. *Aerosol Air Qual. Res.* 14(6): 1752-1762.

11. Eder B.K., Davis J.M. and Bloomfield P. (1994). An automated classification scheme designed to better elucidate the dependence of ozone on meteorology. *J. Appl. Meteor.* 33: 1182-1199.

12. Eder, B., Bash, J., Foley, K. and Pleim, J. (2014).Incorporating principal component analysis into air quality model evaluation. *Atmos. Environ.* 82: 307-315.

13. Fang, G.C., Lin, S.J., Chang, S.Y. and Chou, C.C. (2009). Effect of typhoon on atmospheric particulates in autumn in central Taiwan. *Atmos. Environ.* 43: 6039-6048.

14. Huang, Y., Li, T., Wu, C., He, Z., Japenga, J., Deng, M. and Yang, X. (2015). An integrated approach to assess heavy metal source apportionment in peri-urban agricultural soils. *J. Hazard. Mater.* 299: 540-549.

15. Iodice, P., Adamo, P., Capozzi, F., Di Palma, A., Senatore, A., Spagnuolo, V. and Giordano, S. (2016). Air pollution monitoring using emission inventories combined with the moss bag approach. *Sci. Total Environ.* 541: 1410-1419.

16. Kuebler, J., Russell, A. G., Hakami, A., Clappier, A. and Van den Bergh, H. (2002). Episode selection for ozone modelling and control strategies analysis on the Swiss Plateau. *Atmos. Environ.* 36: 2817-2830.

17. Lai, I.C., Lee, C.L. and Huang, H.C. (2016). A new conceptual model for quantifying transboundary contribution of atmospheric pollutants in the East Asian Pacific rim region.

Environ. Int. 88: 160-168.

18. Li, S. and Wen, J. (2014). A model-based fault detection and diagnostic methodology based on PCA method and wavelet transform. *Energ. Buildings* 68: 63-71.
19. Luo, X. S., Xue, Y., Wang, Y. L., Cang, L., Xu, B. and Ding, J. (2015). Source identification and apportionment of heavy metals in urban soil profiles. *Chemosphere* 127: 152-157.
20. Maheras P. (1984). Weather-type classification by factor analysis in the Thessaloniki area. *J. Climatol.*4: 437-443.
21. Mari, M., Sánchez-Soberón, F., Audí-Miró, C., van Drooge, B. L., Soler, A., Grimalt, J. O., and Schuhmacher, M. (2016). Source apportionment of inorganic and organic PM in the ambient air around a cement plant: Assessment of complementary tools. *Aerosol Air Qual. Res.* 16: 3230-3242.
22. Maryon R.H. and Storey A.M. (1985). A multivariate statistical model for forecasting anomalies of half-monthly mean surface pressure. *J. Climatol.* 5: 561-578.
23. Meyer, E.L., Baldridge, K.W., Chu, S. and Cox, W.M. (1997). Choice of Episodes to Model: Considering Effects of Control Strategies on Ranked Severity of Prospective Episodes Days. *Air & Waste Management Association's 90th Annual Meeting & Exhibition* 97-MP112.01.
24. Oh, H.R., Ho, C.H., Kim, J., Chen, D., Lee, S., Choi, Y.S., Chang, L.S. and Song, C.K. (2015). Long-range transport of air pollutants originating in China: A possible major cause of multi-day high-PM10 episodes during cold season in Seoul, Korea. *Atmos. Environ.* 109: 23-30.
25. Perez, P. and Reyes, J. (2002). Prediction of maximum of 24-h average of PM10 concentrations 30 h in advance in Santiago, Chile. *Atmos. Environ.* 36: 4555-4561.
26. Rutllant, J. and Garreaud, R. (1995). Meteorological air pollution potential for Santiago, Chile: towards an objective episode forecasting. *Environ. Monit. Assess.* 34: 223-244.

27. Shi, G. L., Feng, Y. C., Wu, J. H., Li, X., Wang, Y. Q., Xue, Y. H. and Zhu, T. (2009). Source identification of polycyclic aromatic hydrocarbons in urban particulate matter of Tangshan, China. *Aerosol Air Qual. Res.* 9: 309-315.

28. Soong, W. K., Hung, C. H., Yuan, C. S. and Yang, H. Y. (2005). Effects of local atmospheric circulation on the formation of high ozone concentration in confined area- A case study in southern Taiwan. *J. Chin. Inst. Environ. Eng.* 15: 163-172.

29. Sun, W., Palazoglu, A., Singh, A., Zhang, H., Wang, Q., Zhao, Z. and Cao, D. (2015). Prediction of surface ozone episodes using clusters based generalized linear mixed effects models in Houston–Galveston–Brazoria area, Texas. *Atmos. Pollut. Res.* 6(2): 245-253.

30. TEPA, (2018). *Support center for air quality models*. Taiwan Environmental Protection Administration, https://aqmc.epa.gov.tw/.

31. U.S. EPA (1991). *Guideline for Regulatory Application of Urban Airshed Models*, EPA-450/4-91- 013, US Environmental Protection Agency, Atmospheric Sciences, Research Laboratory, Research Triangle Park, NC.

32. Viana, M., Querol, X., Alastuey, A., Gil, J.I. and Menéndez, M. (2006). Identification of PM sources by principal component analysis (PCA) coupled with wind direction data. *Chemosphere* 65: 2411-2418.

33. Yao, L., Yang, L., Yuan, Q., Yan, C., Dong, C., Meng, C. and Wang, W. (2016). Sources apportionment of PM2.5 in a background site in the North China Plain. *Sci. Total Environ.* 541: 590-598.

34. Yu, T. Y. (2013). Identification of source regions of PM_{10} with backward trajectory-based statistical models during PM_{10} episodes. *Environ. Monit. Assess.* 185: 6465-6475.

35. Yu, T. Y. and Chang, I. C. (2006). Spatiotemporal features of severe air pollution in northern Taiwan. *Environ. Sci. Pollut. R.* 13: 268-275

36. Yu, T.Y. and Chang, L.F.W., 2000, Selection of the scenarios of ozone pollution at southern Taiwan area utilizing principal component analysis. *Atmos. Environ.* 34: 4499-4509.

37. Zhang, H., Palazoglu, A., Zhang, X., Zhang, W., Zhao, Z., Sun, W. and Liu, S. (2014). Prediction of surface ozone exceedance days using PCA with a non-parametric T2 control limit. *Chemometrics Intell. Lab. Sys.* 133: 42-48.

Figure Captions

Figure 1 Locations of ambient air quality monitoring stations over Zhuoshui River

Figure 2 The monthly mean PM_{10} concentrations of monitoring stations

Figure 3 Distribution of daily mean PM_{10} concentrations in dry and wet seasons

Figure 4 Relationship between PC1 score and percentage of exceedance for daily PM_{10} standard and average numbers of exceeding daily PM_{10} standard

Figure 5 The relationships between hourly PM_{10} concentrations and meteorogoical parameters in July, 2013 at Synguang station

Figure 1 Locations of ambient air quality monitoring stations over Zhuoshui River

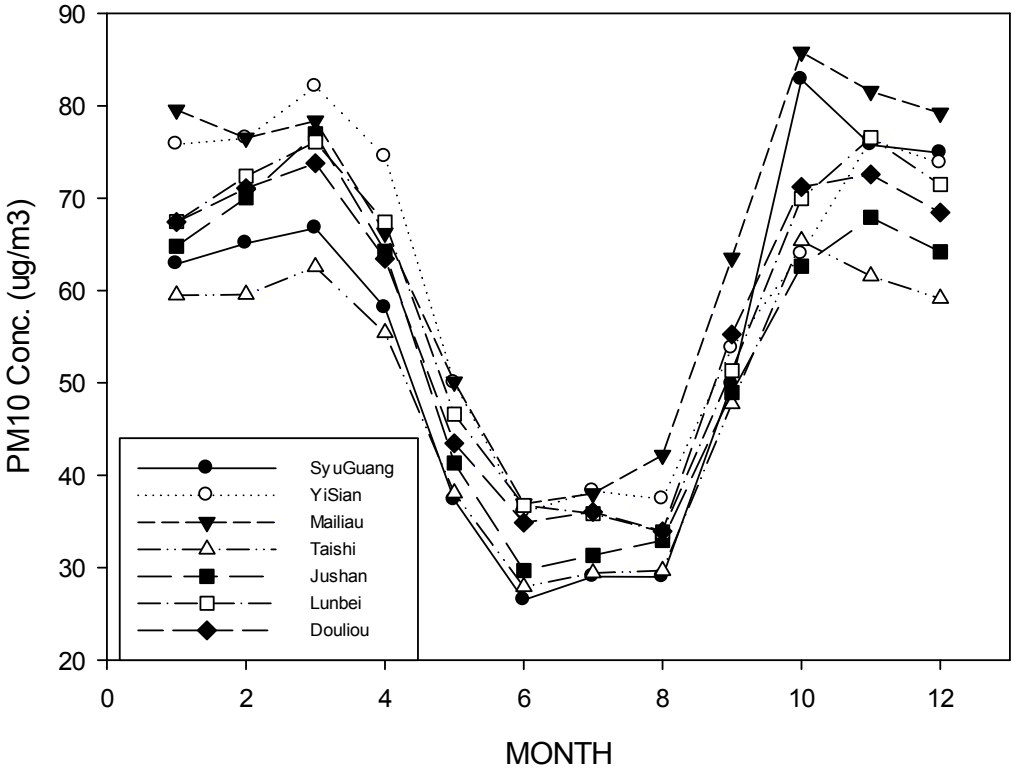

Figure 2 The monthly mean PM_{10} concentrations of monitoring stations

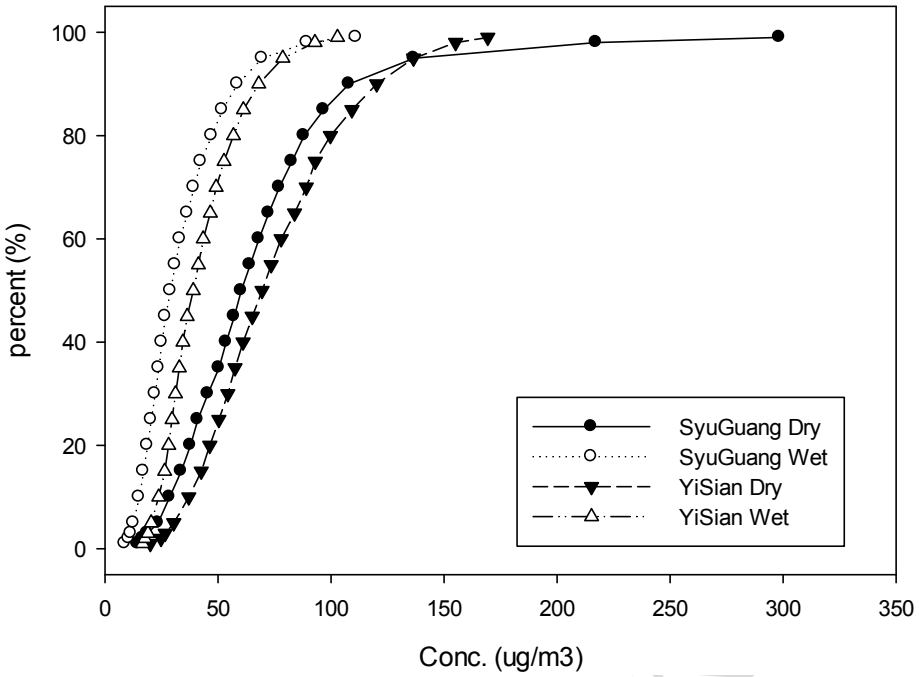

a. Syuguang and Yisian

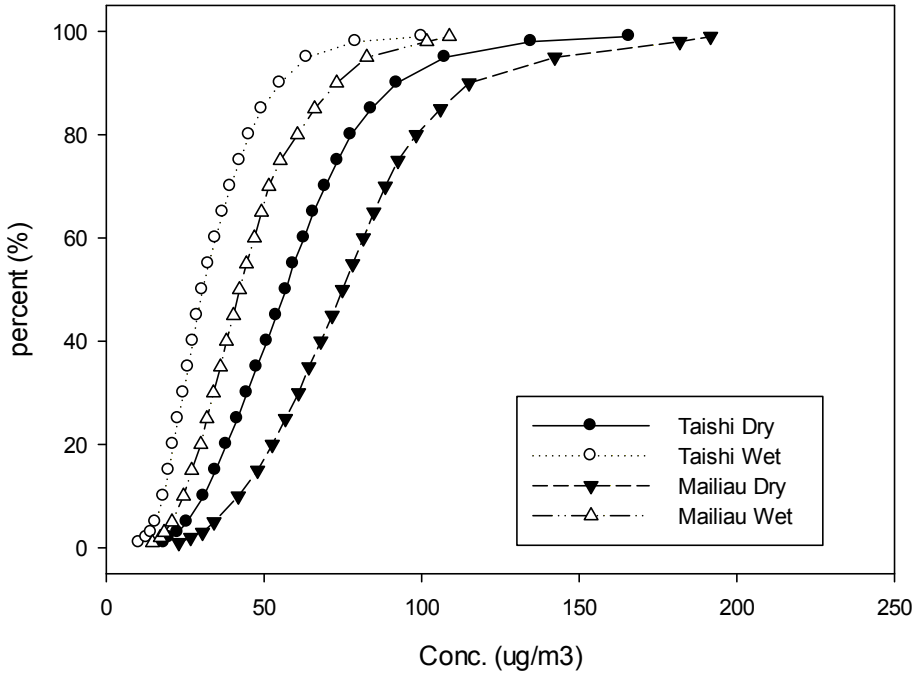

b.Taishi and Mailiau

Figure 3 Distribution of daily mean PM_{10} concentrations in dry and wet seasons

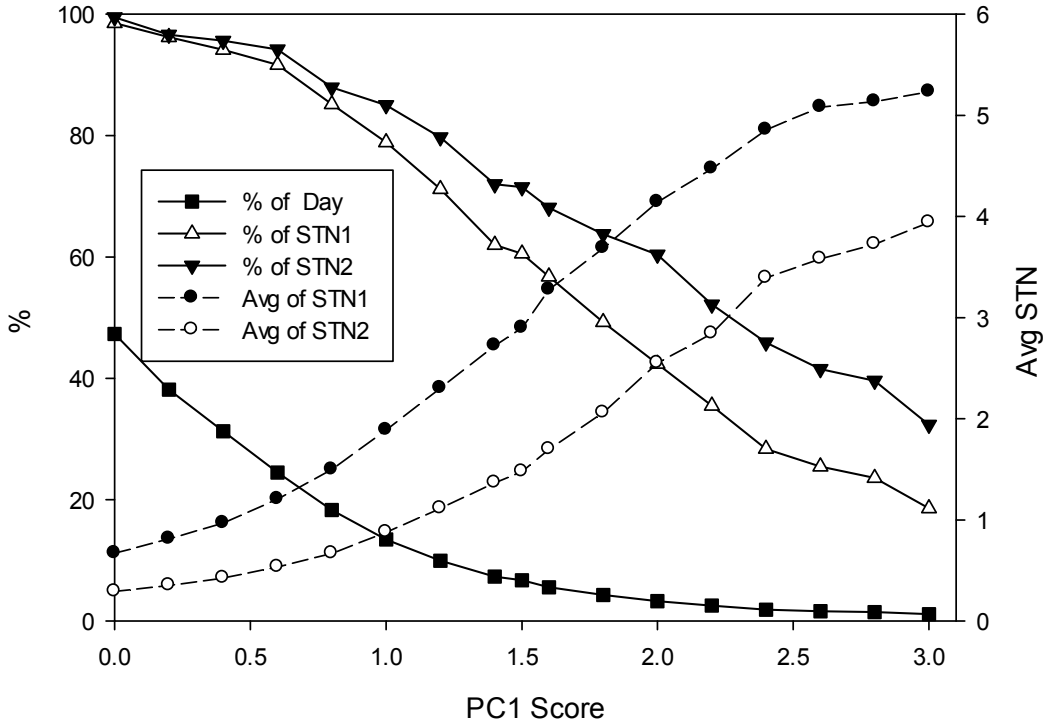

Figure 4 Relationship between PC1 score and percentage of exceedance for daily PM_{10} standard and average numbers of exceeding daily PM_{10} standard
PC1: the component scores of the first component

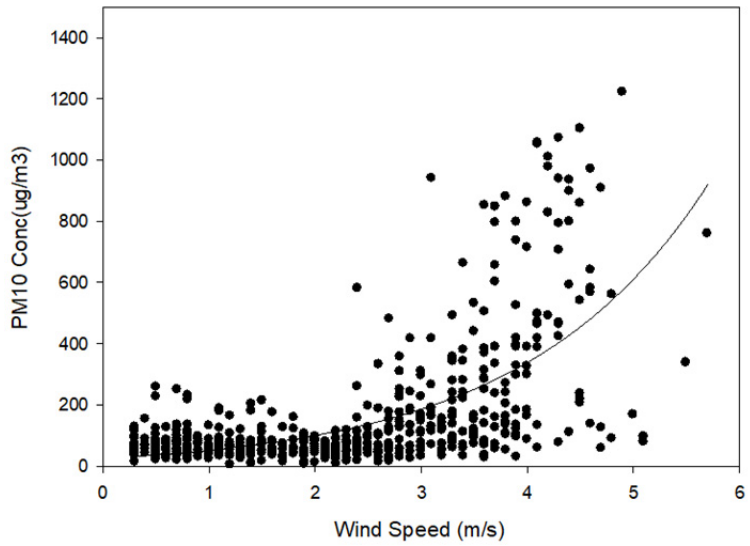

a.wind speed

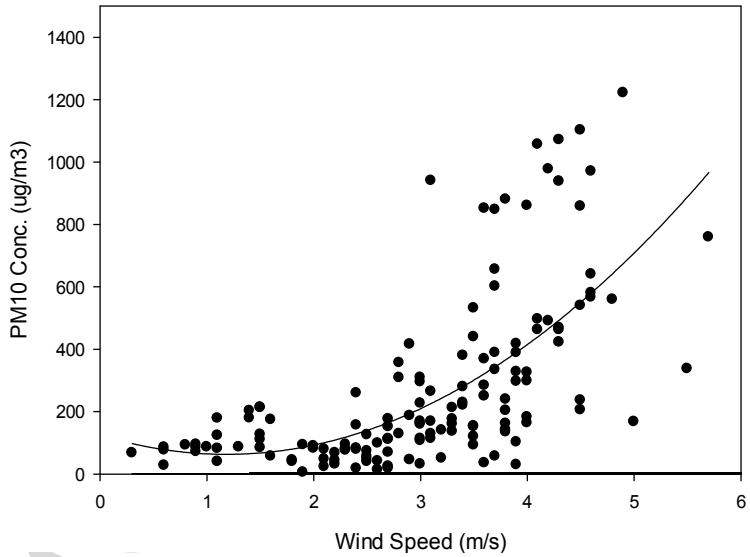

b. wind speed (July 21-27, 2013)

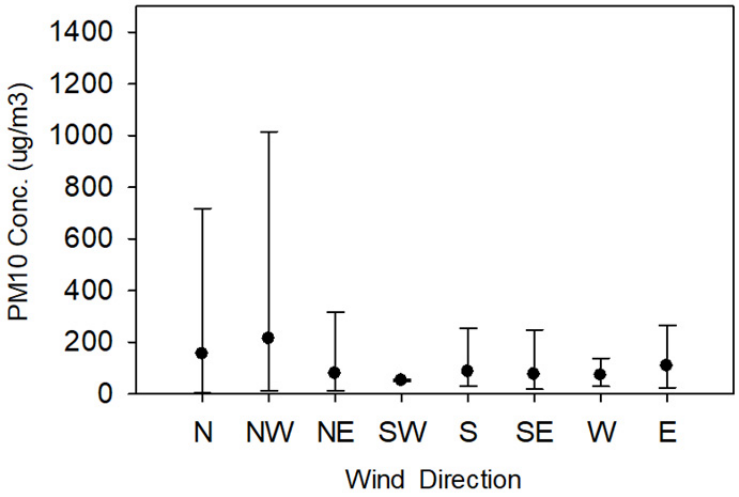

c.Wind direction

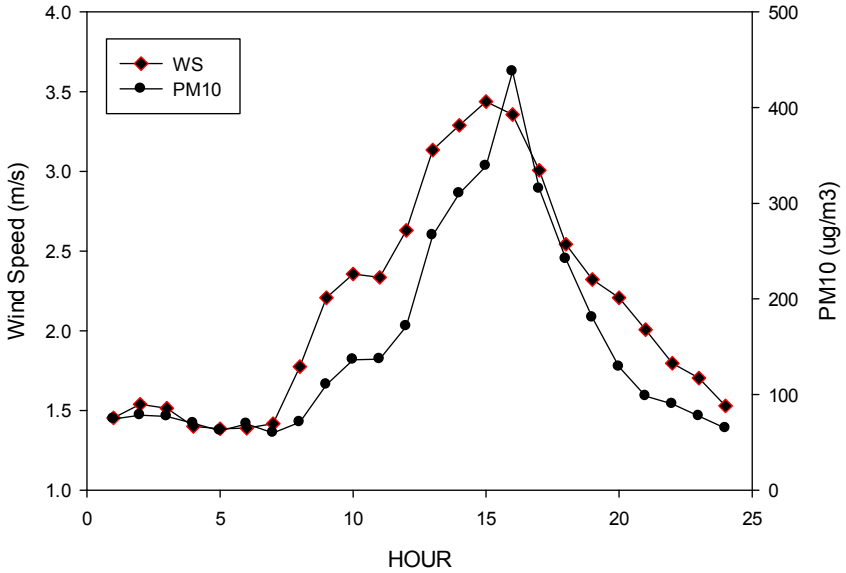

d. the realtioship between wind speed and PM10 levels at distinct hours

Figure 5. The relationships between hourly PM10 concentrations and meteorogoical parameters in July, 2013 at Synguang station

Table Captions

Table 1 Eigenvalues and explained variances for principal components

Principal Component	Eigenvalues	Explained variances (%)
1	4.57	65.3
2	.89	12.7
3	.55	7.9
4	.32	4.6
5	.29	4.1
6	.23	3.3
7	.14	2.0

Table 2 Factor loadings between monitoring stations and principal components

	Components				
Stations	1	2	3	4	5
Syuguang	.783	.260	-.497	.022	.178
Yisian	.829	-.274	-.200	.132	-.414
Douliou	.888	.082	.085	-.293	-.116
Lunbei	.848	-.352	-.142	.111	.230
Taishi	.834	.330	.135	-.267	.019
Mailiau	.723	.490	.314	.367	-.009
Jushan	.739	-.515	.351	-.004	.138

Table 3 River fugitive dust episodes oevr Zhuoshui River that component scores of the first component (PC1) are over 3

Date	Syuguang	Yisian	Douliou	Lunbei	Taishi	Mailiau	Jushan	PC1
2013/2/25	172.2	197.5	175.3	186.3	121.5	126.6	161.3	3.85
2013/10/22	417.0	96.3	192.8	95.7	127.0	155.7	80.0	3.36
2013/10/25	276.0	114.6	185.0	94.6	214.5	168.2	84.9	3.51
2013/11/17	209.8	99.7	161.2	127.3	245.0	179.6	111.3	3.66
2013/11/18	154.6	107.5	141.2	135.0	238.4	144.1	126.0	3.30
2013/11/20	216.3	188.9	157.8	163.2	120.4	124.8	127.5	3.45
2013/12/27	243.1	173.3	230.3	159.2	193.1	183.4	142.8	4.79
2014/1/4	165.7	179.8	164.2	140.8	141.5	163.5	121.0	3.38
2014/1/5	149.8	155.5	159.0	159.9	149.3	148.2	130.5	3.31
2014/1/18	415.6	137.1	263.1	128.1	215.0	215.5	102.3	5.28
2014/1/21	345.4	142.5	246.2	132.0	367.9	224.1	113.3	6.05
2015/2/5	252.1	124.9	175.9	112.4	135.0	223.5	106.3	3.44
2015/11/26	400.5	194.7	227.2	57.4	139.4	189.5	49.4	3.85
2015/12/16	259.8	163.3	181.4	117.0	138.2	169.1	106.7	3.51
2016/12/27	384.7	54.8	238.5	77.2	88.3	217.0	48.2	3.02
2017/10/29	333.7	165.1	47.3	208.1	238.6	71.4	153.5	3.75
2017/10/30	299.0	165.5	53.4	173.5	185.9	63.6	138.8	3.00
2017/11/4	264.4	202.3	33.6	190.3	211.3	38.9	166.8	3.19

Table 4 The screening results of river fugitive dust episodes over Zhuoshui River (daily mean PM_{10}, μg m^{-3})

Items	Date	Syuguang	Yisian	Douliou	Lunbei	Taishi	Mailiau	Jushan
1	2017/10/12	58.5	40.8	51.3	55.8	90.3	86.7	55.4
1	2017/10/13	289.3	63.1	41.5	230.8	145.2	129.8	42.7
1	2017/10/14	29.4	23.6	24.6	19.6	26.1	32.8	17.7
1	2017/10/15	17.8	21.9	15.0	16.0	**	28.3	13.4
1	2017/10/16	35.8	30.7	33.9	38.0	**	52.0	38.4
2	2013/10/22	417.0	96.3	192.8	95.7	127.0	155.7	80.0
2	2013/10/23	373.3	91.6	141.3	93.9	88.4	116.3	83.7
2	2013/10/24	328.0	132.4	207.3	90.8	127.4	97.5	61.3
2	2013/10/25	276.0	114.6	185.0	94.6	214.5	168.2	84.9
2	2013/10/26	165.0	89.3	114.0	91.5	124.8	106.4	81.2
3	2013/10/2	183.5	64.7	92.3	76.1	84.6	73.8	130.9
3	2013/10/3	158.0	74.1	104.9	119.3	84.6	78.8	146.7
3	2013/10/4	225.5	53.0	73.2	64.8	64.1	65.8	106.4
3	2013/10/5	260.1	82.4	52.6	47.0	60.0	83.3	167.1
3	2013/10/6	138.0	47.7	47.5	**	28.0	34.1	80.4

** The number of effective hours are lower than 16

Table 5 Relationships between synoptic weather patterns, daily mean PM_{10} and component scores of the first component

synoptic weather patterns	ratio %	Syuguang	Yisian	Douliou	Lunbei	Taishi	Mailiau	Jushan	PC1	Lunbei WS(m/s)
Northeast monsoon and peripheral circulation of the typhoon	0.9	172.3	79.5	115.9	83.5	91.7	108.7	71.1	1.14	3.7
Peripheral circulation of the typhoon	1.3	84.9	71.6	77.2	58.1	51.6	79.7	56.9	-0.12	3.0
High-pressure circulation mixing with a warm sector	0.2	84.0	86.0	83.2	76.2	72.6	88.9	71.5	0.41	1.9
Pacific High Pressure	2.0	80.0	76.3	81.2	79.7	65.8	78.0	81.2	0.30	2.5
Pacific High Pressure stretching westerly	2.9	76.7	94.8	79.8	81.1	68.4	74.2	70.3	0.33	2.5
High-pressure recirculation	16.3	76.5	93.5	78.0	84.3	63.2	77.5	76.7	0.34	2.1
Strong northeast monsoon	13.3	75.9	73.1	74.8	65.3	66.4	92.6	67.1	0.10	4.0
Standard northeast monsoon	21.7	59.8	63.9	66.7	66.8	60.8	76.9	64.4	-0.17	3.6
Weak northeast monsoon	14.6	65.8	74.9	70.6	73.8	60.6	77.1	70.3	0.03	2.8

The numbers except for ratio, PC1 and wind speed (WS) are PM_{10} levels

Table 6 Average component scores of distinct synoptic weather patterns and wind speed categories

Synoptic Weather	Average component scores of PC1		Probability (%)	
	Wind speed			
	<3.5 m/s	>=3.5 m/s	<3.5 m/s	>=3.5m/s
Frontal passage	-0.55	-0.59	2.12	0.47
Ahead of warm front	0.10	-0.25	4.24	1.10
Strong northeast monsoon	0.02	0.15	4.79	8.48
Standard northeast monsoon	0.05	-0.33	9.18	12.48
Weak northeast monsoon	0.11	-0.33	11.85	2.75
Off-shored high pressure I	0.10	-0.48	2.20	1.02
Off-shored high pressure Ⅱ	0.29	-0.44	1.02	0.16
High pressure reflux	0.52	0.55	13.66	2.67
Pacific High Pressure system stretching westerly	0.33	0.34	2.75	0.16
Southwest flow	-1.51	-1.99	0.16	0.08
Coastal front	0.20	-0.86	0.86	0.24
Pacific High Pressure system	0.17	1.28	1.81	0.24
South flow	-0.10	-0.14	3.69	0.94
Northeast monsoon and peripheral circulation of the typhoon	0.00	1.95	0.39	0.55
Peripheral circulation of the typhoon	-0.34	0.38	0.86	0.39
Northeast monsoon and South China rain area move eastward	0.52	-1.18	1.41	1.73